2018

A model-based design optimization strategy for ground source heat pump systems with integrated photovoltaic thermal collectors

Lei Xia
University of Wollongong, lx873@uowmail.edu.au

Zhenjun Ma
University of Wollongong, zhenjun@uow.edu.au

Georgios Kokogiannakis
University of Wollongong, gkg@uow.edu.au

Zhihua Wang
University of Wollongong, zhihua@uow.edu.au

Shugang Wang
Dalian University of Technology, shugang@uow.edu.au

A model-based design optimization strategy for ground source heat pump systems with integrated photovoltaic thermal collectors

Abstract

This paper presents a model-based design optimization strategy for ground source heat pump systems with integrated solar photovoltaic thermal collectors (GSHP-PVT). A dimension reduction strategy using Morris global sensitivity analysis was first used to determine the key design parameters of the GSHP-PVT system. A model-based design optimization strategy was then formulated to identify the optimal values of the key design parameters to minimize the life-cycle cost (LCC) of the GSHP-PVT system, in which an artificial neural network (ANN) model was used for performance prediction and a genetic algorithm (GA) was implemented as the optimization technique. A simulation system of a GSHP-PVT system developed using TRNSYS was used to generate necessary performance data for dimension reduction analysis, and for the ANN model training and validation. The results showed that the ANN model used was able to provide an acceptable prediction of the operational cost of the GSHP-PVT system. In comparison to two baseline cases, the 20-year life cycle cost (LCC) of the GSHP-PVT system studied can be decreased by 20.1% and 10.2% respectively, when using the optimal values determined by the proposed optimization strategy. This design optimization strategy can be potentially adapted to formulate the design optimization strategies for GSHP systems an d other building energy systems.

Disciplines

Engineering | Science and Technology Studies

Publication Details

Xia, L., Ma, Z., Kokogiannakis, G., Wang, Z. & Wang, S. (2018). A model-based design optimization strategy for ground source heat pump systems with integrated photovoltaic thermal collectors. Applied Energy, 214 178-190.

A model-based design optimization strategy for ground source heat pump systems with integrated photovoltaic thermal collectors

Lei Xia[a], Zhenjun Ma[a,*], Georgios Kokogiannakis[a], Zhihua Wang[a,b], Shugang Wang[c]

[a]Sustainable Buildings Research Centre, University of Wollongong, NSW, 2522, Australia

[b]School of Human Settlements and Civil Engineering, Xi'an Jiaotong University, 710049, China

[c]Faculty of Infrastructure Engineering, Dalian University of Technology, 116024, China

*Email: zhenjun@uow.edu.au

Abstract: This paper presents a model-based design optimization strategy for ground source heat pump systems with integrated solar photovoltaic thermal collectors (GSHP-PVT). A dimension reduction strategy using Morris global sensitivity analysis was first used to determine the key design parameters of the GSHP-PVT system. A model-based design optimization strategy was then formulated to identify the optimal values of the key design parameters to minimize the life-cycle cost (LCC) of the GSHP-PVT system, in which an artificial neural network (ANN) model was used for performance prediction and a genetic algorithm (GA) was implemented as the optimization technique. A simulation system of a GSHP-PVT system developed using TRNSYS was used to generate necessary performance data for dimension reduction analysis, and for the ANN model training and validation. The results showed that the ANN model used was able to provide an acceptable prediction of the operational cost of the GSHP-PVT system. In comparison to two baseline cases, the 20-year life cycle cost (LCC) of the GSHP-PVT system studied can be decreased by 20.1% and 10.2%

respectively, when using the optimal values determined by the proposed optimization strategy. This design optimization strategy can be potentially adapted to formulate the design optimization strategies for GSHP systems and other building energy systems.

Keywords: Design optimization; Dimension reduction; GSHP; PVT; Artificial neural network; Genetic algorithm.

Nomenclature

A_1, A_2 coefficients

A_c floor area of the building (m^2)

A_{pvt} total area of the PVT collector (m^2)

B distance between boreholes (m)

C coefficient

C_b drilling and grouting cost per meter ($/m)

C_{EB} electricity buy price ($/kWh)

C_{ES} electricity sell price ($/kWh)

C_{ma} annual maintenance cost of the system ($/year)

C_{op} annual operation cost of the system ($/year)

C_p cost of U-tube per meter ($/m)

C_{PVT} price of PVT collectors per square meter ($/$m^2$)

D outer diameter of water tube (mm)

DC residual cost ($)

E_{con} annual electricity consumption of the system (kWh/year)

E_{gen} annual electricity generation of the system (kWh/year)

EE elementary effect ($)

e coefficient

F_R heat removal efficiency factor

f coefficient

G incident solar radiation on the PVT collector (W/m^2)

h_c overall convection heat loss coefficient (W/m^{2}K)

h_r radiation heat loss coefficient (W/m^{2}K)

h_w convection heat loss coefficient due to the wind (W/m^{2}K)

H_b borehole depth (m)

IC initial cost ($)

j number of design parameters

k number of elementary effects

k_{abs} absorber thermal conductivity (W/m.K)

k_{ins} back insulation thermal conductivity (W/m.K)

k_g grout material thermal conductivity (W/m.K)

L_{abs} absorber plate thickness (mm)

L_b total borehole length (m)

LCC life cycle cost ($)

L_{ins} back insulation thickness (mm)

L_p total U-tube length (m)

MC maintenance cost ($)

M_{ma} annual maintenance cost per square meter ($/m^2)

m_{pvt} circulating fluid mass flow rate per PVT tube (kg/s)

N_g number of glass covers

N_s number of simulations

N number of time steps

Q_u useful thermal energy (kW)

OC operation cost ($)

P_c probability of crossover

P_m probability of mutation

RC replacement cost ($)

r discount rate

r_b borehole radius (m)

r_o U-tube outer radius (m)

T temperature (K)

$(UA)_e$ edge loss coefficient – area product (W/m.K)

U_b bottom loss coefficient (W/m^2 K)

U_L overall loss coefficient (W/m^2 K)

U_e edge loss coefficient (W/m^2 K)

U_t top loss coefficient (W/m^2 K)

V_{TK} volume of water tank (L)

W water tube spacing (mm)

x_c half shank space (m)

α absorptance

γ temperature coefficient

ε_g emittance of glass

ε_p emittance of PV plate

η efficiency

μ mean value of the elementary effects

σ' Stefan's Boltzmann constant ($W/m^2 K^4$)

σ standard deviation of the elementary effects

τ transmittance

Δ increment

Subscripts

amb ambient

c cell

GHE ground heat exchanger

HP heat pump

in inlet

Pu pump

PVT photovoltaic thermal collector

mp mean plate

pv photovoltaic

r reference

TK tank

th thermal

WH water heater

1. Introduction

Ground source heat pump (GSHP) systems as one of the energy efficient and environmentally friendly technologies have been receiving wide attention [1, 2]. Solar photovoltaic thermal (PVT) collector is another promising technology which can produce both electricity and thermal energy simultaneously [3]. Appropriate integration of PVT collectors with GSHP systems could result in an efficient system that can provide cooling and heating as well as domestic hot water (DHW), offset the need of grid electricity and alleviate ground thermal imbalance.

A significant number of studies have been performed to couple solar thermal collectors with GSHP systems and focused on the system performance evaluation [4-8], optimal design and intelligent control [9-13]. Recently, there was an increasing number of studies focusing on the integration of GSHP systems with PVT collectors, among which most of them were concentrated on the performance evaluation and performance comparison of GSHP-PVT systems with conventional heating and cooling systems under a given PVT collector area

[14-18]. For example, Bakker et al. [14] simulated the performance of a GSHP-PVT system in a dwelling with a floor area of 132 m^2 in the Netherlands. The results showed that a PVT collector with an area of 54 m^2 can cover the heating demand and nearly all electricity demand of the dwelling while keeping the long-term average ground temperature constant. Entchev et al. [15] and Canelli et al. [16] investigated the performance of a GSHP-PVT system to provide cooling, heating and DHW in load sharing applications in Ottawa (Canada) and Napoli (Italy), respectively. The results from Entchev et al. [15] showed that the GSHP-PVT system can result in an overall energy saving of 58% in comparison to a conventional system with boilers and chillers. The results from Canelli et al. [16] showed that, compared to a conventional system, the primary energy savings of the GSHP-PVT system were 53.1%. Brischoux and Bernier [17] examined the performance of a GSHP-PVT system for space heating and DHW heating. The results showed that the coupled GSHP-PVT system, in which the PVT collectors were cooled by the heat transfer fluid from the borehole, can provide 7.7% more electricity annually with a higher seasonal performance factor in comparison to an uncoupled system. The results from these studies demonstrated that the GSHP-PVT system can result in a better energy performance in comparison to conventional heating and cooling systems and/or stand-alone GSHP systems. However, the results from these studies were highly dependent on the size of the PVT collector used.

Proper design of hybrid GSHP-PVT systems, however, has not been extensively studied. To date, only a limited number of studies examined the effect of key design parameters on the energy performance of hybrid GSHP-PVT systems. Bertram et al. [19] investigated the key

design parameters, such as location, wind velocity, size of PVT collector and total GHE length, on the energy performance of a hybrid GSHP system with unglazed PVT collector. Xia et al. [20] examined the influence of PVT collector size on the performance of a GSHP-PVT system in a heating dominated residential building, and determined the optimal PVT collector size for the case study building through an economic analysis. However, there is no study in the public domain that has optimally sized the whole GSHP-PVT system. The high initial investment of both GSHP and PVT collector makes the short-term economics of such systems unattractive and the optimization of the key design parameters of the GSHP-PVT system therefore becomes more important.

Artificial neural network (ANN) has been widely used to analyze complex engineering problems [21, 22]. The main advantage of ANN models is that they can simulate multivariable problems with complex relationships among the variables and can approximate the implicit non-linear relationship between input and output variables by means of ‘learning’ with the training data [22, 23]. Genetic algorithm (GA) is known as an efficient optimization algorithm that can provide good solutions with random initializations [24, 25]. The use of ANN and GA to formulate optimization problems for buildings and building energy systems has been reported in a number of studies. For instance, Kalogirou [26] developed a design optimization method that combined ANN and GA to size the major design parameters of solar systems. The results showed that the optimal solutions obtained by using this proposed method increased the life cycle savings of 4.9% and 3.1% when subsidized and non-subsidized fuel prices were used respectively, as compared to the solutions obtained by

using the traditional trial-and-error method. Magnier and Haghighat [27] developed a multi-objective optimization method to optimize the thermal comfort and energy consumption of a residential house. In this method, a simulation-based ANN was used to characterize building behaviors and a GA was used to find the optimal solutions. The results from these studies indicated that the integration of ANN and GA could be potentially utilized to solve complex optimization problems and can result in reasonable solutions.

In this study, a model-based design optimization strategy was developed to determine the optimal values of the key design parameters of a GSHP-PVT system, in which an artificial neural network (ANN) model was used for performance prediction and a genetic algorithm (GA) was used as the optimization technique. By integrating ANN with GA, the complex nonlinear characteristics of the system could be learned and predicted by the ANN model, and the design problem of the hybrid GSHP-PVT system could be potentially solved. To facilitate the design optimization, a dimension reduction strategy using Morris global sensitivity analysis was used to determine the key design parameters of the GSHP-PVT system. A simulation system of the GSHP-PVT system was also developed and used to generate necessary data for the dimension reduction analysis and ANN model training and validation. The methodology used to formulate this design optimization strategy can be adapted to develop advanced design optimization strategies for hybrid GSHP-PVT systems suitable for real applications. The results obtained from this study could also be used to guide and facilitate the design of hybrid GSHP-PVT systems.

2. System development and simulation

2.1 System development

A GSHP system integrated with a water-based PVT collector, as shown in Fig. 1, was used to provide heating and cooling demand, and domestic hot water (DHW) for heating-dominated buildings. The hybrid system consisted of a PVT collector, a water tank with immersed heat exchangers, a water-to-water heat pump unit, three water circulation pumps, a vertical ground heat exchanger (GHE) loop, an indoor air-handling unit (AHU) and an electric water heater. This system can operate under different modes, as described in Table 1, to provide functional requirements to the house through on-off control of the isolation valves.

In this system, the GSHP system is mainly used to provide a fraction of heating demand and the total cooling demand of the building. The thermal energy collected from the PVT collector is used to provide DHW, a fraction of heating demand of the building during the heating period and to recharge the ground during the transition period in order to achieve an annual thermal balance of the ground. The electricity generated by the PVT collector can be used to drive the operation of the GSHP-PVT system while the extra electricity generation can be exported to the grid.

2.2 System modeling

To facilitate the development of the design optimization strategy, a virtual simulation system of this GSHP-PVT system was developed using TRNSYS [28]. This simulation system was used to generate the performance data of the system under different values of the

design parameters to support the dimension reduction analysis and the ANN performance model training and validation.

The major component models used to develop the simulation system were the standard models provided in the TRNSYS library. They included a water-to-water heat pump model (Type 927), a vertical U-tube GHE model (Type 557a), a water tank model with immersed heat exchangers (Type 534), water circulation pump models (Type 110 for variable speed pumps and Type 114 for constant speed pumps), and an electric water heater model (Type 6).

In order to simulate the performance of both glazed and unglazed water-based PVT collectors, a new PVT model (i.e. Type 500) was created by combining the mathematical models presented by Anderson et al. [29] and Fudholi et al. [30].

The thermal performance of the PVT collector was simulated using the Hottel-Whillier equations. The useful thermal energy (Q_u) of the PVT collector is calculated using Eq. (1) [31], in which the overall collector heat loss coefficient (U_L) is the sum of the edge (U_e), top (U_t) and bottom (U_b) loss coefficients [22].

$$Q_u = A_{pvt} F_R \left[(\tau\alpha)_{PV} \cdot G - U_L (\mathrm{T}_{in} - \mathrm{T}_{amb}) \right] \quad (1)$$

where A_{pvt} is the collector area, F_R is the heat removal efficiency factor, $(\tau\alpha)_{PV}$ is the transmittance-absorptance of the PV cell, G is the incident solar radiation on the PVT collector, and T_{in} and T_{amb} are the PVT collector inlet fluid temperature and the ambient temperature, respectively.

The edge and bottom loss coefficients can be determined using Eqs. (2) and (3), respectively [31]. For glazed and unglazed PVT collector, the top loss coefficient (Ut) is

calculated using Eqs. (4) [30] and (5) [29], respectively.

$$U_e = \frac{(UA)_e}{A_{pvt}} \tag{2}$$

$$U_b = \frac{k_{ins}}{L_{ins}} \tag{3}$$

$$U_t = \left[\frac{N_g}{\frac{C}{T_{mp}} \left(\frac{T_{mp} - T_{amb}}{N_g + f} \right)^e} \frac{1}{h_w} \right]^{-1} + \frac{\sigma' \left(T_{mp} + T_{amb} \right) \left(T_{mp}^2 + T_{amb}^2 \right)}{(\varepsilon_p + 0.00591 N h_w)^{-1} + \frac{2N_g + f - 1 + 0.133\varepsilon_p}{\varepsilon_g} - N} \tag{4}$$

$$U_t = h_r + h_c \tag{5}$$

where $(UA)_e$ is the edge loss coefficient-area product, and k_{ins} and L_{ins} are the thermal conductivity and the thickness of the back insulation respectively, N_g is the number of the glass covers, h_w is the convection heat loss coefficient due to the wind, σ' is the Stefan-Boltzmann constant, ε_p is the plate emittance, ε_g is the glass emittance, T_{mp} is the mean plate temperature, *C*, *f*, *e* are the coefficients which can be obtained following the method provided by Fudholi et al. [30], and h_r and h_c are the radiation heat loss and overall convection heat loss coefficients respectively which can be determined using the methodology provided in Anderson et al. [29].

The thermal efficiency (η_{th}) and electrical efficiency (η_{pv}) of the PVT collector can be calculated using Eqs. (6) and (7), respectively.

$$\eta_{th} = \frac{Q_u}{A_{pvt} G} \tag{6}$$

$$\eta_{pv} = \eta_r (1 - \gamma \cdot (T_c - T_r)) \tag{7}$$

where η_r is the reference efficiency of the PV module, γ is the temperature coefficient, T_c

is the cell temperature, and T_r is the reference temperature.

In the simulation, the PVT water pump was switched on when the incident solar radiation was over 300 W/m^2 and the PVT mean plate temperature was 5 ^{o}C higher than the average water temperature in the water tank. The ground recharge was implemented when the water temperature in the tank during the transition period was over 30 ^{o}C. The amount of the thermal energy to be recharged into the ground was estimated based on the annual heat extraction and heat rejection from the GSHP system simulated using the same GSHP-PVT system but without using the ground recharge. Once the thermal energy transferred to the ground can maintain the annual ground thermal balance, the heat energy generated from the PVT collector during the transition period was used for DHW heating only. During the cooling period, the heat energy generated from the PVT collector was only used for DHW heating. During the heating period, the heat generated by the PVT collector was used for DHW heating and in the meantime, was used for space heating when the building had a heating demand and the water temperature in the water tank was over 40^{o}C. The electric water heater was only used to heat the water from the water tank when there was a DHW demand and the water temperature in the tank was lower than the required temperature. The GSHP was used when there was a cooling demand or when there was a heating demand and the water temperature in the water tank was below 40^{o}C. The supply and return chilled water temperatures of the GSHP system were assumed to be 7^{o}C and 12^{o}C in the cooling mode, and 45^{o}C and 40^{o}C in the heating mode, respectively.

3. Dimension reduction using Morris global sensitivity analysis

As there are many design parameters (Fig. 2) influencing the performance of the hybrid GSHP-PVT system, a dimension reduction strategy was first used to identify the key design parameters with a great impact on the performance of the GSHP-PVT system in order to facilitate the design optimization. As shown in Fig. 3, the dimension reduction process started with the generation of the input matrix by sampling the candidate design parameters based on the design constraints. The input matrix was used to design the simulation scenarios to determine the annual performance data of the GSHP-PVT system on the basis of the simulation system presented in Section 2. The simulation results were then used to calculate the LCC of the GSHP-PVT system based on the cost function estimator and the resulted LCC were used to generate the element effects, and the mean values and standard deviations of the element effects. The last step was to evaluate the influence of each candidate design parameter on the objective function by comparing the mean values and standard deviations in order to determine the key design parameters.

3.1 Morris sensitivity analysis method

In this study, Morris global sensitivity analysis was utilized for the dimension reduction as this method can handle a large number of parameters with a low computational cost, and can achieve a good compromise between the accuracy and efficiency [32]. The minimum number of simulations required for Morris sensitivity analysis method is determined by Eq. (8) [33].

$$N_s = k \cdot (j+1) \tag{8}$$

where N_s is the number of simulations, k is the number of the elementary effects per parameter, and j is the number of design parameters.

From Morris analysis, two sensitivity indicators, i.e. mean value (μ) and standard deviation (σ) of the absolute values of the elementary effects as defined in Eqs. (9) and (10) respectively, can be obtained [33]. The mean value is used to estimate the main influence of the input parameter on the output while the standard deviation is used to evaluate the interactions among the parameters or the non-linear effects. In the Morris method, the factors are generally represented by a plane (μ, σ) in order to compare their relative influence [34].

$$\mu = \sum_{i=1}^{k} \left| EE_i \right| / k \tag{9}$$

$$\delta = \sqrt{\sum_{i=1}^{k} \left| EE_i - \mu \right|^2 / k} \tag{10}$$

where EE is the elementary effect, and k is the number of the elementary effects investigated for each parameter.

The elementary effect EE is derived from a model $y=y(x_1 ,\ldots, x_j)$ with j input parameters, i.e. $x_1,\ldots, x_j$. The EE for the i^{th} input parameter at the k^{th} sampling point is calculated by Eq. (11) [35].

$$EE_i^{(k)} = \frac{y(\mathrm{x}_1^{(k)}, \mathrm{x}_2^{(k)} ..., \mathrm{x}_{i-1}^{(k)}, \mathrm{x}_i^{(k)} + \Delta, \mathrm{x}_{i+1}^{(k)}, ..., \mathrm{x}_j^{(k)}) - y(\mathrm{x}_1^{(k)}, ..., \mathrm{x}_j^{(k)})}{\Delta} \tag{11}$$

The successful use of Morris sensitivity analysis method is dependent on proper sampling of each input parameter within its defined range. In this study, Latin hypercube sampling method was used for this purpose, which can generate a certain number of discretized values within the constraints defined for each parameter to improve the efficiency

of the Morris method [34].

3.2 Objective function

The objective function used in the dimension reduction was the 20-year life cycle cost (LCC) of the GSHP-PVT system in the net present value. The LCC generally includes the initial cost (IC), operation cost (OC), maintenance cost (MC), replacement cost (RC) and residual cost (DC), as expressed in Eq. (12) [36, 37]. In this study, the initial cost was determined by Eq. (13), in which the upfront costs of GHEs, PVT collector and water tank were determined using Eqs. (14)-(16), respectively. The 20-year operational cost was determined using Eq. (17) [37], in which the annual operational cost was determined using Eq. (18). The 20-year maintenance cost was determined using Eq. (19) [37], in which the annual maintenance cost was determined using Eq. (20). In this study, the replacement cost was not considered and the residual cost was also not considered due to the lack of the information on calculating the salvage values of the GSHP system and the PVT collector.

$$LCC = IC + OC + MC + RC + DC \tag{12}$$

$$IC = IC_{GHE} + IC_{HP} + IC_{PVT} + IC_{TK} + IC_{Pu} + IC_{WH} \tag{13}$$

$$IC_{GHE} = C_p L_p + C_b L_b \tag{14}$$

$$IC_{PVT} = C_{PVT} A_{PVT} \tag{15}$$

$$IC_{Tk} = A_1 V_{TK} + A_2 \tag{16}$$

$$OC = C_{op} \cdot \left(\frac{1-(1+r)^{-n}}{r}\right) \tag{17}$$

$$C_{op} = \begin{cases} \sum_{i=1}^{N} (E_{con}^{i} - E_{gen}^{i}) \cdot C_{EB}, & if\ E_{con}^{i} > E_{gen}^{i} \\ \sum_{i=1}^{N} (E_{con}^{i} - E_{gen}^{i}) \cdot C_{ES}, & if\ E_{con}^{i} < E_{gen}^{i} \end{cases} \quad (18)$$

$$MC = C_{ma} \cdot (\frac{1-(1+r)^{-n}}{r}) \quad (19)$$

$$C_{ma} = M_{ma} \cdot A_c \quad (20)$$

where C_p is the cost of the U-tube per meter, L_p is the total U-tube length within all boreholes, C_b is the drilling cost and grouting cost per meter, L_b is the total borehole length, C_{PVT} is the cost of the PVT collector per square meter, A_{PVT} is the area of the PVT collector, V_{TK} is the volume of the water tank, A_1 and A_2 are the coefficients which were determined based on the tank prices of various volumes, r is the discount rate, C_{op} is the annual operational cost, E_{con}^{i} and E_{gen}^{i} are the electricity consumption and generation of the system at the i^{th} simulation time step, respectively, C_{EB} and C_{ES} are the electricity buy and sell prices per kWh, respectively, N is the total number of simulation time steps, C_{ma} is the annual maintenance cost of the system, M_{ma} is the annual maintenance cost per square meter, A_c is the air conditioned floor area of the building, and the subscripts *GHE*, *HP*, *PVT*, *TK*, *Pu* and *WH* represent the ground heat exchanger, heat pump unit, photovoltaic thermal collector, water tank, water pump and water heater, respectively.

3.3 Constraints

In this study, the following constraints were applied in the dimension reduction. The minimum area of the PVT collector was determined based on the thermal energy required to recharge the ground in order to achieve an annual thermal balance. The amount of the thermal

energy to be recharged into the ground was estimated based on the simulation assumptions described in Section 2.2. The maximum value was determined based on the north rooftop area of the building. The variation ranges of the other design parameters of the PVT collector were determined based on the data used in previous studies [29, 30, 38-44], and the details are presented in Section 5.

The capacity of the GSHP system was determined to satisfy the heating and cooling demand of the building at the design condition. The estimated total length of the vertical GHEs was associated with the design load and the design heat flux through GHEs. The acceptable range of the heat flux is dependent on the thermal conductivity of the soil on the site [45]. The variation ranges of the geometrical parameters such as the number of boreholes, borehole depth, and the distance between boreholes were determined based on the recommended values from practical engineering projects [45-47].

The volume of the water tank was determined based on the estimated daily average hot water consumption of the building according to the Australian and New Zealand Standard for Heated Water Services [48].

4. Development of the model-based design optimization strategy

4.1 Outline of the optimization strategy

The primary aim of the design optimization was to determine the optimal values of the key design parameters to minimize the 20-year life cycle cost (LCC) of the GSHP-PVT system in terms of the net present value. The outline of the optimization strategy is illustrated in Fig. 4, which was developed using a model-based approach and the key parameters

identified through the dimension reduction. In this strategy, an ANN model was used to predict the system performance under different working conditions and a GA was used as the optimization technique to identify the optimal solution of the optimization problem to minimize the cost function. The same cost function and constraints as those used in the dimension reduction strategy were used as the optimization objective and optimization constraints, respectively.

4.2 Development of the ANN performance model

In this study, a multi-layer feedforward ANN model, as shown in Fig. 5, was used as the performance model to facilitate the design optimization. This model consisted of neurons in the input layer for the key design variables determined through the dimension reduction, two hidden layers and one output layer with the annual operational cost of the system. The model structure was determined through trial and error tests to ensure that it can provide a relatively fast and good convergence. Latin hypercube sampling method was also used to generate a relatively small but a representative number of scenarios with different combinations of the input parameters (i.e. key design parameters). The design scenarios were then simulated using the simulation system developed in order to generate a number of datasets for the ANN model training and validation. The ANN model was trained using the Levenberg–Marquardt (LM) and Bayesian regularization algorithms.

5. Performance test and evaluation

5.1 Setup of the test

A typical Australian house [49] with a floor area of 248 m^2 and a conditioned floor area

of 200 m^2 was used as the case building for evaluating the performance of the proposed design optimization strategy. Fig. 6 illustrates the building model developed using DesignBuilder and the resulted building load profile based on the International Weather for Energy Calculations (IWEC) of Melbourne, Australia. It can be seen that the annual heating demand of the house was significantly higher than the cooling demand under the Melbourne climatic conditions. Based on the heating and cooling demand of the house at the design condition, the water-to-water heat pump unit can then be determined. Table 2 lists the major parameters of the heat pump unit considered, which was selected according to the product specification available from a manufacturer [50].

Table 3 summarizes the cost values of the input parameters used to calculate the 20-year LCC of the GSHP-PVT system. The material costs of the PVT collector, the costs of the GHE U-tube pipe, the water circulation pumps, the water tank and the electric water heater were referred to the wholesale price provided on the alibaba.com website [51]. The drilling and grouting costs of the GHEs were obtained from a previous study [47], and the cost of the heat pump unit was sourced from a manufacturer [41]. The electricity price for residential buildings in Melbourne considered was 0.26 $/kWh and any extra electricity generated by the PVT collector can be sold back to the grid with a price of 0.05 $/kWh according to the feed-in tariff scheme in Victoria 2016 [52]. The discount rate was chosen according to the value provided by Trading Economics [53].

The constraints for the candidate design parameters used are summarized in Table 4, which were determined based on the design constraints presented in Section 3.3, weather and

soil conditions, and the house cooling and heating demand.

As each design case has a different fluid mass flow rate, the three water pumps used were sized for each case based on the design fluid mass flow rate and the calculated pipe network resistance. In this study, the PVT circulation pump and the water pump in the GSHP source side used were constant speed pumps while that used in the GSHP load side was a variable speed pump. The design heat flux through the GHEs obtained from the study of Lhendup et al. [54], was used to estimate the total length of the vertical GHEs, due to the same soil condition. The total number of boreholes was associated with the borehole depth. During the simulation, DHW was set to be required between 7:00 and 10:00, and 17:30 and 21:30 with a flow rate of 16 L/h [55].

The values of other parameters used in this case study are summarized in Table 5, which were maintained constant in this study. The PVT related parameters were derived from the study of Fudholi et al. [30] and the GHE related parameters were derived from Lhendup et al. [54].

5.2 Dimension reduction results

In order to carry out the dimension reduction analysis, the models for glazed and unglazed PVT collector were first validated using the data reported by Anderson et al. [29], and the validation results are presented in Fig. 7. It can be observed that the model predicted thermal efficiency and the electrical efficiency of the PVT collector against the ratio of the temperature difference (T_{in}-T_{amb}) to the global radiation incident on the collector surface (G) generally agreed well with the measured values. The maximum relative deviations between

the model predicted and measured thermal efficiency were 1.0% and 4.5%, while those between the predicated and measured electrical efficiency were 1.9% and 2.1% for the glazed and unglazed PVT collector, respectively. The validation results indicated that the models for the PVT collector used can provide an acceptable estimation and can satisfy the purpose of this study.

The relative sensitivities of the 16 candidate design parameters as listed in Table 4 to the objective function (i.e. 20-year LCC) of the hybrid GSHP-PVT system were then analyzed. For all candidate design parameters, two discretized values were used for the PVT type (i.e. glazed and unglazed), and five discretized values were used for the other parameters, which were generated using the Latin hypercube sampling method within their corresponding constraints. The total number of the simulation cases was then determined using Eq. (8).

The results from the Morris sensitivity analysis are shown in Fig. 8. It can be seen that the area of the PVT collector (i.e. factor 1) was the most influential design parameter on the LCC of the GSHP-PVT system with the highest mean value and standard deviation. The second most influential design parameter was the PVT type (i.e. factor 2), followed by the ratio of the tube width to the spacing (i.e. factor 8), the borehole depth (i.e. factor 10) and the circulation fluid mass flow rate per PVT tube (i.e. factor 9). The remaining parameters can be considered as the parameters with a less impact on the LCC of the GSHP-PVT system and the constant values (see Table 6) determined based on the existing studies and design practices were therefore used in the following design optimization.

5.3 Performance evaluation of the design optimization strategy

5.3.1 ANN model validation

In this study, the total number of the datasets used for the ANN model training was 30 times of the number of the key design variables, which was considered to be sufficient to accurately sample the search space of the design variables [56]. Another 30 datasets were used to validate the effectiveness of the ANN model. Each dataset corresponded to a simulation scenario with different combinations of the key design parameters identified through the dimension reduction analysis. Therefore, a total number of 180 scenarios were designed and simulated using the simulation system developed in Section 2.

Fig. 9 presents the results of the ANN model validation. It can be observed that the model predicted annual operational costs of the GSHP-PVT system agreed well with the results generated from the simulation system with R^2 of 0.998. This indicated that the ANN model used was able to provide an acceptable prediction of the system performance within the range of the training data covered. It is worthwhile to note that the accuracy of the ANN model is highly dependent on the training data used and the use of the ANN model beyond the range of the training data used may result in significant errors.

5.3.2 Design optimization results

The five key design parameters were then globally optimized using the model-based optimization strategy. The maximum number of the generations used in the optimization was 300, which was determined based on trial and error tests. The variances of the fitness function during the optimization process are shown in Fig. 10. It can be observed that the

fitness value was gradually stable after 250 generations. The optimal solutions of the design problem identified are summarized in Table 7 and are compared with those of two baseline design cases. In the baseline case I, the key design parameters were obtained from an earlier study [20] and the unglazed PVT collector was used. In the baseline case II, the glazed PVT collector was used instead of using the unglazed PVT collector while the remaining design parameters were the same as those of the baseline case I. The other design parameters except the five key design parameters used in the three design cases can be found in Tables 2, 5 and 6. From Table 7, it can be seen that the baseline case II with the glazed PVT collector can reduce 11.1% of the 20-year LCC of the GSHP-PVT system as compared to the baseline case I using the unglazed PVT collector. The optimal design identified by the proposed strategy was able to reduce the 20-year LCC by 20.1% and by 10.2%, in comparison to the baseline case I and baseline case II, respectively. From Table 7, it can also be observed that the total initial cost and the operational cost of the system under the baseline design case I were both higher than that under the optimal design case. The optimal design case saved the initial cost of $7,515 and the operational cost of $9,341 respectively, as compared to the baseline design case I. The baseline design case II saved $541 more operational cost as compared to the optimal design case, but required $8,141 more initial cost. The annual CO_2 emissions of the system under the optimal design case and the two baseline design cases were also presented in Table 7. The CO_2 emission factor for the consumption of the purchased electricity used was 1.08 kg CO_2/kWh [57]. It can be seen that the optimal design case and the baseline design case II were able to reduce the annual CO_2 emission of 1625.3 kg (29.5%) and 1731.3 kg

(31.4%), respectively, when compared to the baseline design case I. The annual CO_2 emission of the optimal design case was slightly higher than that of the baseline design case II.

Fig. 11 presents the details of the total initial cost, monthly operational cost, monthly electricity consumption and monthly electricity generation of the GSHP-PVT system when using the optimal design and baseline design parameters. It can be seen that the major difference in the initial cost of the system between the optimal design case and baseline design cases was the cost of the PVT collector. The cost of the PVT collector under the baseline design case I and baseline design case II were $7,515 and $8,141 higher than that under the optimal design case, respectively, mainly due to the use of a larger PVT collector area and a more compact arrangement of the water tubes (i.e. a relatively high D/W ratio) (Fig 11a)). The operational cost of the GSHP-PVT system under the optimal design case was always lower than that under the baseline design case I (Fig. 11 b)). The main reason for the lower operational cost was mainly because, in the optimal design case, the glazed PVT collector produced more thermal energy, in comparison to the baseline design case I using the unglazed PVT collector and even with a larger PVT collector area. This results in a lower electrical demand for producing DHW (Fig. 11 c)). Although the baseline design case I generated more electricity monthly (Fig. 11 d)) in comparison to the optimal design case, the gap between the electricity buy and sell prices made this benefit less obvious. The operational cost of the system under the baseline design case II was lower than that under the optimal design case in particular during the transition period (i.e. April and November). The difference in the monthly electricity consumption of the system between the optimal design

case and the baseline design case II was relatively small (Fig. 11 c)). However the monthly electricity generation of the system under the baseline case II was always higher than that under the optimal design case (Fig. 11 d)), due to the use of a larger PVT collector area. It is worthwhile to note that, in this analysis, the priority of the thermal energy collected from the PVT collector was used for the ground recharging during the transition period. Therefore, the power consumption during the transition period was mainly resulted by the use of the electric heater for DHW supply. The results from the performance test and evaluation demonstrated the effectiveness of the proposed optimal design strategy for hybrid GSHP-PVT systems. The ANN model used was able to provide an acceptable estimation of the system performance and the GA was able to find the near optimal solutions of the optimization problem. However, the proposed strategy is generally computationally intensive in comparison to traditional rule-of-thumb design methods, due to the requirement of the extensive data for ANN model training and validation. This would be an obstacle of applying this strategy to real-world design. However, this design optimization strategy and the associated results can be used to facilitate the development of advanced and efficient design strategies that can be readily used in practice.

6. Sensitivity study

To understand the sensitivity of the optimization results to the PV cell price, drilling cost and electricity price, another simulation exercise was carried out in this study. Fig. 12 shows the variation in the 20-year LCC of the GSHP-PVT system with the optimal design parameters under different price combinations. It can be seen that the 20-year LCC increased

significantly with the increase in the PV cell price and drilling cost, but decreased with the increase of the electricity sell price. The 20-year LCC did not show a remarkable sensitivity to the change of the electricity buy price. Table 8 summarizes the optimization results with the variations of different economic parameters. It is noted that the glazed PVT collector was identified as the optimal PVT collector type for all scenarios. From the results, it can be concluded that the change of the PV cell price, drilling cost and electricity buy price did not affect the optimization results significantly since the optimal values of the other four design parameters almost remained constant. However, the optimal area of the PVT collector increased from 54 m^2 to 78 m^2 when the electricity sell price increased from 0.05 $/kWh to 0.30 $/kWh, which confirmed that a larger PVT collector area is economically beneficial to the hybrid GSHP-PVT system if the electricity generated by the system can be sold back to the grid with a higher price.

7. Conclusions

This paper presented a new design optimization strategy for a hybrid ground source heat pump system integrated with photovoltaic thermal collectors (GSHP-PVT). In this strategy, an artificial neural network (ANN) model was used for performance prediction and a genetic algorithm (GA) was used as the optimization technique. The 20-year life cycle cost (LCC) of the GSHP-PVT system was used as the optimization objective.

This proposed design optimization strategy was evaluated through a case study. The ANN model was trained and validated using the datasets created through a number of numerical simulations, based on the key design parameters identified by a dimension

reduction strategy using Morris global sensitivity analysis method. The results showed that the ANN model was able to provide acceptable estimations of the annual operational cost of the GSHP-PVT system with R^2 of 0.998. The optimization results showed that the 20-year LCC of the GSHP-PVT system under the optimal design case was 20.1% and 10.2% lower than those of the two baseline design cases I and II, respectively. The sensitivity of the optimization results to the variations in the PV cell price, drilling cost and electricity buy and sell prices was also analyzed. It was shown that the PV cell price, drilling cost and electricity buy price had a limited impact on the overall optimization results. However, the electricity sell price greatly affected the optimal PVT collector area. This study demonstrated that the combination of ANN and GA could be potentially useful to formulate the design optimization strategies for hybrid GSHP-PVT systems. The proposed design optimization strategy could be potentially adapted to formulate the design optimization strategy for other complex energy systems.

This study aimed to fill the research gap on the design optimization of hybrid GSHP-PVT systems. However, the design optimization strategy developed is generally computationally intensive.

References

[1] Yang H, Cui P, Fang Z. Vertical-borehole ground-coupled heat pumps: A review of models and systems. Appl Energy. 2010; 87: 16-27.

[2] Huang S, Ma Z, Wang F. A multi-objective design optimization strategy for vertical

ground heat exchangers. Energy Build. 2015; 87: 233-42.

[3] Chow TT. A review on photovoltaic/thermal hybrid solar technology. Appl Energy. 2010; 87: 365-79.

[4] Dai L, Li S, DuanMu L, Li X, Shang Y, Dong M. Experimental performance analysis of a solar assisted ground source heat pump system under different heating operation modes. Appl Therm Eng. 2015; 75: 325-33.

[5] Reda F, Arcuri N, Loiacono P, Mazzeo D. Energy assessment of solar technologies coupled with a ground source heat pump system for residential energy supply in Southern European climates. Energy. 2015; 91: 294-305.

[6] Emmi G, Zarrella A, De Carli M, Galgaro A. An analysis of solar assisted ground source heat pumps in cold climates. Energy Convers Manage. 2015; 106: 660-75.

[7] Esen H, Esen M, Ozsolak O. Modelling and experimental performance analysis of solar-assisted ground source heat pump system. J Exp Theor Artif Intell. 2017; 29: 1-17.

[8] Chen X, Yang H. Performance analysis of a proposed solar assisted ground coupled heat pump system. Appl Energy. 2012; 97: 888-96.

[9] Kjellsson E, Hellstrom G, Perers B. Optimization of systems with the combination of ground-source heat pump and solar collectors in dwellings. Energy. 2010; 35: 2667-73.

[10] Zhao J, Chen Y, Lu S, Cui J. Optimization of serial combined system of ground-coupled heat pump and solar collector. Trans of Tianjin Univ. 2009; 15: 37-42.

[11] Verma V, Murugesan K. Optimization of solar assisted ground source heat pump system for space heating application by Taguchi method and utility concept. Energy Build. 2014; 82:

296-309.

[12] Reda F, Laitinen A. Different strategies for long term performance of SAGSHP to match residential energy requirements in a cold climate. Energy Build. 2015; 86: 557-72.

[13] Razavi SH, Ahmadi R, Zahedi A. Modeling, simulation and dynamic control of solar assisted ground source heat pump to provide heating load and DHW. Appl Therm Eng. 2018; 129: 127-44.

[14] Bakker M, Zondag H, Elswijk M, Strootman K, Jong M. Performance and costs of a roof-sized PV/thermal array combined with a ground coupled heat pump. Sol energy. 2005; 78: 331-9.

[15] Entchev E, Yang L, Ghorab M, Lee E. Performance analysis of a hybrid renewable microgeneration system in load sharing applications. Appl Therm Eng. 2014; 71: 697-704.

[16] Canelli M, Entchev E, Sasso M, Yang L, Ghorab M. Dynamic simulations of hybrid energy systems in load sharing application. Appl Therm Eng. 2015; 78: 315-25.

[17] Brischoux P, Bernier M. Coupling PV/T collectors with a ground-source heat pump system in a double U-tube borehole. ASHRAE Winter Conf. Orlando, 2016.

[18] Emmi G, Zarrella A, De Carli M. A heat pump coupled with photovoltaic thermal hybrid solar collectors: A case study of a multi-source energy system. Energ Convers Manage. 2017; 151: 386-99.

[19] Bertram E, Glembin J, Rockendorf G. Unglazed PVT collectors as additional heat source in heat pump systems with borehole heat exchanger. Energy Procedia. 2012; 30: 414-23.

[20] Xia L, Ma Z, Kokogiannakis G. Performance Simulation of a Ground Source Heat Pump

System Integrated with Solar Photovoltaic Thermal Collectors for Residential Applications. The 15th Inter Conf of IBPSA. San Francisco, 2017.

[21] Kalogirou SA. Applications of artificial neural-networks for energy systems. Appl Energy. 2000; 67: 17-35.

[22] Wong SL, Wan KK, Lam TN. Artificial neural networks for energy analysis of office buildings with daylighting. Appl Energy.2010; 87: 551-7.

[23] Esen H, Inalli M, Sengur A, Esen M. Performance prediction of a ground-coupled heat pump system using artificial neural networks. Expert Syst with Appl. 2008; 35: 1940-48.

[24] Wang JJ, Jing YY, Zhang CF. Optimization of capacity and operation for CCHP system by genetic algorithm. Appl Energy. 2010; 87: 1325-35.

[25] Ma Z, Wang S. Supervisory and optimal control of central chiller plants using simplified adaptive models and genetic algorithm. Appl Energy. 2011; 88: 198-211.

[26] Kalogirou SA. Optimization of solar systems using artificial neural-networks and genetic algorithms. Appl Energy. 2004; 77: 383-405.

[27] Magnier L, Haghighat F. Multiobjective optimization of building design using TRNSYS simulations, genetic algorithm, and Artificial Neural Network. Build Environ. 2010; 45: 739-46.

[28] TRNSYS. The Transient Energy System Simulation Tool, http://www.trnsys.com/; 2017 [Accessed 20 September 2017].

[29] Anderson TN, Duke M, Morrison G, Carson JK. Performance of a building integrated photovoltaic/thermal (BIPVT) solar collector. Sol Energy. 2009; 83: 445-55.

[30] Fudholi A, Sopian K, Yazdi MH, Ruslan MH, Ibrahim A, Kazem HA. Performance analysis of photovoltaic thermal (PVT) water collectors. Energ Convers Manage. 2014; 78: 641-51.

[31] Duffie JA, Beckman WA. Solar engineering of thermal processes. Wiley New York; 2013.

[32] Tian W. A review of sensitivity analysis methods in building energy analysis. Renew Sust Energy Rev. 2013; 20: 411-19.

[33] Saltelli A, Tarantola S, Campolongo F, Ratto M. Sensitivity analysis in practice: a guide to assessing scientific models. John Wiley & Sons; 2004.

[34] Sohier H, Piet-Lahanier H, Farges J-L. Analysis and optimization of an air-launch-to-orbit separation. Acta Astronaut. 2015; 108: 18-29.

[35] Heiselberg P, Brohus H, Hesselholt A, Rasmussen H, Seinre E, Thomas S. Application of sensitivity analysis in design of sustainable buildings. Renew Energy. 2009; 34: 2030-36.

[36] Woodward DG. Life cycle costing-theory, information acquisition and application. Int J Proj Manage. 1997; 15: 335-44.

[37] Zhu Y, Tao Y, Rayegan R. A comparison of deterministic and probabilistic life cycle cost analyses of ground source heat pump (GSHP) applications in hot and humid climate. Energy Build. 2012; 55: 312-21.

[38] Farghally H, Ahmed N, El-Madany H, Atia D, Fahmy F. Design and sensitivity analysis of photovoltaic/thermal solar collector. Inter Energy J. 2015; 15: 21-32.

[39] Chow TT, He W, Chan A, Fong K, Lin Z, Ji J. Computer modeling and experimental

validation of a building-integrated photovoltaic and water heating system. Appl Therm Eng. 2008; 28: 1356-64.

[40] Ibrahim A, Fudholi A, Sopian K, Othman MY, Ruslan MH. Efficiencies and improvement potential of building integrated photovoltaic thermal (BIPVT) system. Energ Convers Manage. 2014; 77: 527-34.

[41] Tiwari A, Dubey S, Sandhu G, Sodha M, Anwar S. Exergy analysis of integrated photovoltaic thermal solar water heater under constant flow rate and constant collection temperature modes. Appl Energy. 2009; 86: 2592-97.

[42] Sukesh N, Lakshmisagar P, Kumar G. Heat Transfer Analysis of Fin Performance for PVT Absorber. J Mech Eng Autom. 2015; 5: 1-4.

[43] Chow TT, Pei G, Fong K, Lin Z, Chan A, Ji J. Energy and exergy analysis of photovoltaic–thermal collector with and without glass cover. Appl Energy. 2009; 86: 310-16.

[44] Bhattarai S, Oh J-H, Euh S-H, Kafle GK, Kim DH. Simulation and model validation of sheet and tube type photovoltaic thermal solar system and conventional solar collecting system in transient states. Solar Energy Mater Solar Cells. 2012; 103: 184-93.

[45] Banks D. An introduction to thermogeology: ground source heating and cooling. John Wiley & Sons; 2012.

[46] ASHRAE Handbook. HVAC applications. SI ed. ASHRAE; 2011.

[47] Huang S, Ma Z, Cooper P. Optimal design of vertical ground heat exchangers by using entropy generation minimization method and genetic algorithms. Energ Convers Manage. 2014; 87: 128-37.

[48] Australia Standard. National Plumbing and Drainage: Part 4- Heated Water Services. AS/NZS 350042003.

[49] Craig James SS. US overtakes Australia to build biggest homes. Commsec; 2016. https://www.commsec.com.au/content/dam/EN/ResearchNews/Eco_Insights31.1-0_US_overtakes_Australia_to_build_biggest_homes.pdf.

[50] WaterFurnace. Versatec Ultra NSKW Specification Catalog. 2016. http://www.geoexchange.com.au/download/WaterFurnace%20NSKW%2050HZ%20Aurora-%20S-C2566WN_Specification%20Catalogue.pdf.

[51] Alibaba.com. https://www.alibaba.com/; 2017 [Accessed 20 September 2017].

[52] Commission ES. Minimum Electricity Feed-in Tariff to Apply from 1 January 2016 to 31 December 2016: Final Decision, August; 2015.

[53] Trading Economics. Australia Interest Rate. https://tradingeconom-ics.com/australia/indicators/; 2017 [Accessed 20 September 2017].

[54] Lhendup T, Aye L, Fuller RJ. Thermal charging of boreholes. Renew Energy. 2014; 67: 165-72.

[55] Commonwealth Department of the Environment and Energy. Water Heating Data Collection and Analysis; 2012. http://www.energyrating.gov.au/sites/new.energ-yrating/files/documents/REMP-water-heating_0.pdf.

[56] Conraud-Bianchi J. A methodology for the optimization of building energy, thermal, and visual performance. Masters Abstr Inter, 2008.

[57] Department of the Environment and Energy. National Greenhouse Accounts Facto

-rs; 2017. Available: https://www.environment.gov.au/system/files/resources/5a169bfb-f417-4b00-9b70-6ba328ea8671/files/national-greenhouse-accounts-factors-july-2017.pdf.

[58] Tse K-K, Chow T-T, Su Y. Performance evaluation and economic analysis of a full scale water-based photovoltaic/thermal (PV/T) system in an office building. Energy Build. 2016; 122: 42-52.

Table 1 Potential operation modes of the GSHP-PVT system

Mode	**Description**
PVT for space heating and DHW heating	Using the thermal energy generated from the PVT for space heating and DHW heating.
GSHP for space heating/cooling	Using the GSHP for space heating and cooling.
PVT for ground recharge and DHW heating	Using the thermal energy collected from the PVT to recharge the ground and for DHW heating.
PVT for DHW heating only	Using the thermal energy collected from the PVT for DHW heating only.

Table 2 Summary of major design parameters of the heat pump unit

Parameter	Value
Rated cooling/heating capacity (kW)	12.6/14.4
Rated power consumption (kW)	2.8/2.72
Rated water flow rate (m^3/h)	2.3

Table 3 Input parameters for the calculation of LCC of the system

Component	**Value**	**Source**
PVT collector		
Front glass ($/$m^2$)	9.5	[51]
PV cell ($/$m^2$)	70	[51]
Thermal absorber plate ($/$m^2$)	52	[51]
Water tube in the collector ($/kg)	10	[51]
Back thermal insulation ($/$m^2$)	2.1	[51]
Back plate ($/$m^2$)	6.3	[51]
Manufacturing cost ($/$m^2$)	27	[58]
GSHP system		
U-tube pipe ($/m)		
20 mm outer diameter	0.65	[51]
25 mm outer diameter	1.10	[51]
32 mm outer diameter	1.36	[51]
40 mm outer diameter	2.10	[51]
Drilling ($/m)	75	[47]
Grouting cost ($/m)	8	[47]
Heat pump unit ($/each)	6000	[47]
Others		
Water circulation pump ($/each)	150-500	[51]
Electric water heater ($)	400	[51]
Discount rate (%)	1.5	[53]

Table 4 Candidate design parameters and their constraints used

Controllable parameters		Ranges
1	Area of PVT collectors, A_{pvt} (m^2)	[30, 78]
2	Type of PVT	Glazed or unglazed
3	Absorber plate thickness, L_{abs} (m)	[0.0002, 0.002]
4	Absorber thermal conductivity, k_{abs} (W/m.K)	[50, 300]
5	Insulation thickness, L_{ins} (m)	[0.05, 0.1]
6	Insulation conductivity, k_{ins} (W/m.K)	[0.03, 0.1]
7	Outer diameter of water tube, D (m)	[0.01, 0.02]
8	Ratio of tube width to spacing, D/W	[0.1, 0.7]
9	Circulating fluid mass flow rate per PVT tube, m_{pvt} (kg/s)	[0.002,0.01]
10	Borehole depth, H_b (m)	[40, 120]
11	Borehole distance, B (m)	[3,10]
12	Borehole radius, r_b (m)	[0.05, 0.12]
13	U-tube outer radius, r_o (m)	[0.01, 0.02]
14	Grout material conductivity, k_g (W/m.K)	[0.5, 2.5]
15	Half shank space, x_c (m)	[0, r_b-2r_o]
16	Volume of the water tank, V_{TK} (L)	[200, 400]

Table 5 Summary of constant design parameters of the system used

Parameter		**Value**
PVT related	Absorptivity of plate	0.9
	Emittance of plate	0.95
	Emittance of glass cover	0.88
	Transmittance of glass cover	0.9
	Electrical efficiency at standard conditions (%)	13
	Collector tilt (^{o})	30
GHE related	U-tube material conductivity (W/(m.K))	0.4
	Initial ground temperature (^{o}C)	15.9
	Ground thermal conductivity (W/(m.K))	2.23
	Ground heat capacity (KJ/(m^3 K))	2,300
Other	Power of electric water heater (kW)	15.0

Table 6 Low sensitivity parameters and values used [30, 40, 47]

Parameters	**Values**
Absorber plate thickness (m)	0.002
Absorber thermal conductivity (W/(m.K))	51
Insulation thickness (m)	0.05
Insulation conductivity W/(m.K)	0.045
Outer diameter of water tube (m)	0.012
Borehole distance (m)	8
Borehole radius (m)	0.06
U-tube outer radius (m)	0.0125
Grout material conductivity (W/(m.K))	2.42
Half shank space (m)	0.025
Volume of the water tank (L)	250

Table 7 Comparison between the optimal values identified and those of two baseline cases

Case	Baseline design I	Baseline design II	Optimal design
A_{pvt} (m^2)	66	66	54
PVT type	Unglazed	Glazed	Glazed
D/W	0.4	0.4	0.1
m_{pvt} (kg/s)	0.008	0.008	0.002
H_b (m)	40	40	81
IC ($)	50,434	51,060	42,919
OC ($)	24,725	14,843	15384
MC ($)	8,564	8,564	8,564
20-year LCC ($)	83,723	74,467	66,867
Savings in 20-year LCC (%)	-	11.1	20.1
Annual CO_2 emission (kg/year)	5506.9	3775.6	3881.6
Savings in annual CO_2 emission (%)	-	31.4	29.5

Table 8 The optimization results with the variations of different economic parameters

Parameter	Price	A_{pvt} (m^2)	D/W	m_{pvt} (kg/s)	H_b (m)	20-year LCC ($)
PV cell ($/$m^2$)	40	53	0.13	0.002	82	63,742
	50	53	0.10	0.002	82	65,259
	60	55	0.12	0.003	81	66,141
	70	54	0.10	0.002	81	66,867
	80	55	0.11	0.002	83	67,664
	90	55	0.12	0.003	84	68,688
	100	54	0.10	0.002	83	69,184
Drilling ($/m)	35	56	0.10	0.003	81	61,835
	45	54	0.11	0.003	80	62,966
	55	54	0.11	0.001	82	64,471
	65	54	0.10	0.003	80	65,591
	75	54	0.10	0.002	81	66,867
	85	56	0.10	0.002	82	68,454
	95	56	0.11	0.002	82	69,680
Electricity (buy) ($/kWh)	0.15	54	0.10	0.002	82	66,336
	0.20	53	0.10	0.003	82	66,503
	0.25	54	0.11	0.002	81	66,726
	0.30	54	0.10	0.003	80	67,026
	0.35	55	0.12	0.002	83	67,335
	0.40	54	0.10	0.002	81	67,540
Electricity (sell) ($/kWh)	0.05	54	0.10	0.002	81	66,867
	0.10	68	0.10	0.003	82	65,103
	0.15	75	0.12	0.003	83	63,356
	0.20	77	0.11	0.002	81	61,626
	0.25	78	0.11	0.003	83	59,235
	0.30	78	0.12	0.003	82	58,110

Figure Captions

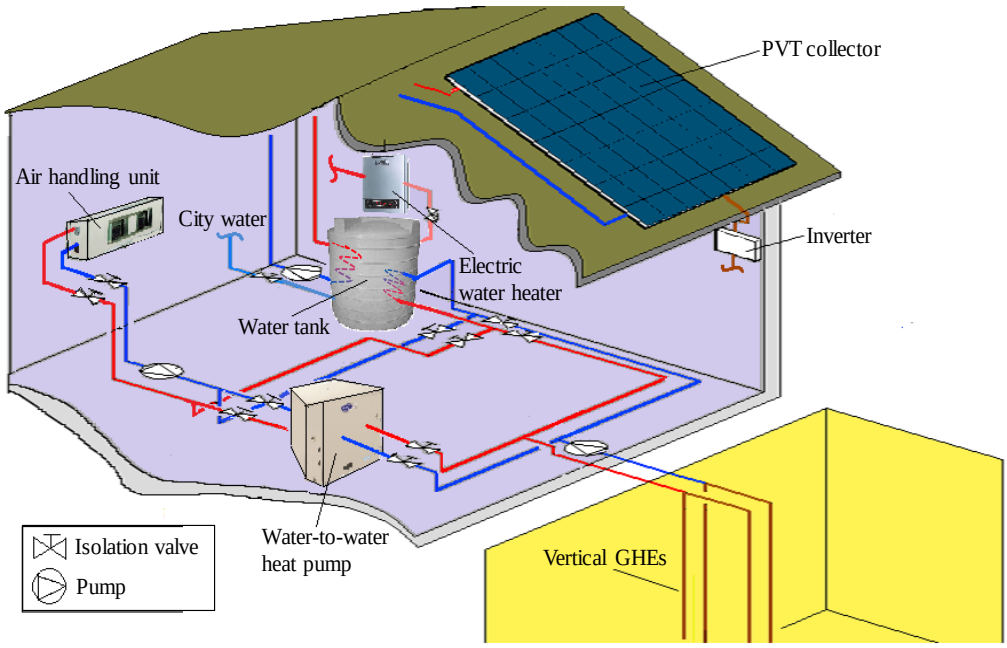

Fig. 1 Schematic of the proposed GSHP-PVT system.

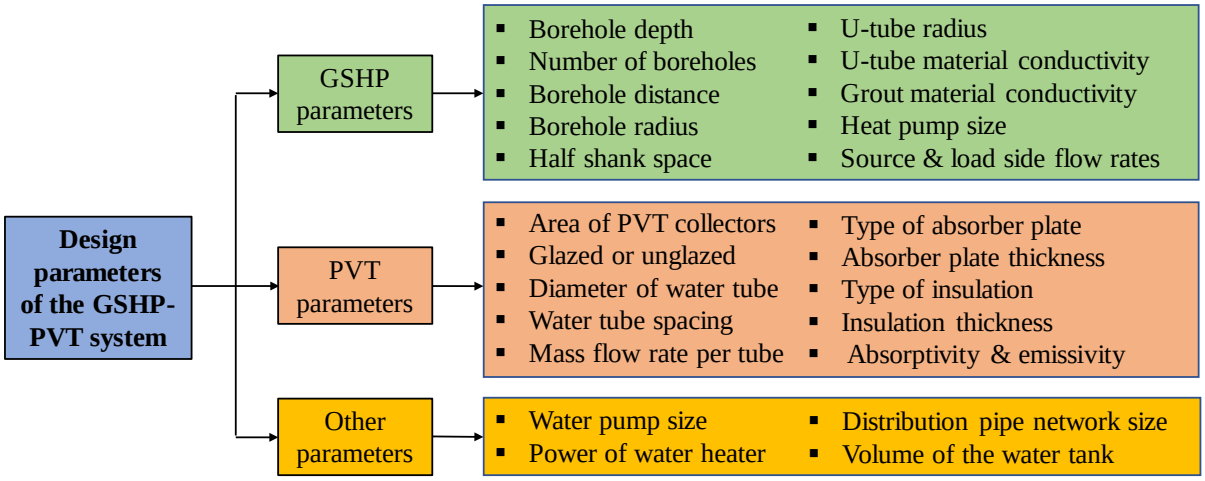

Fig. 2 Parameters that may affect the performance of a GSHP-PVT system.

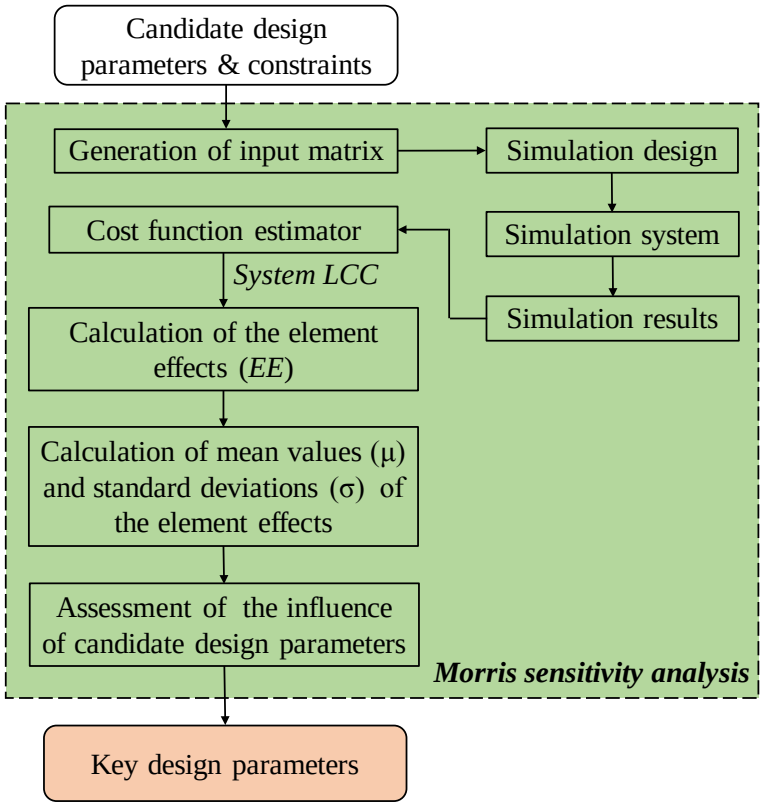

Fig. 3 Dimension reduction process.

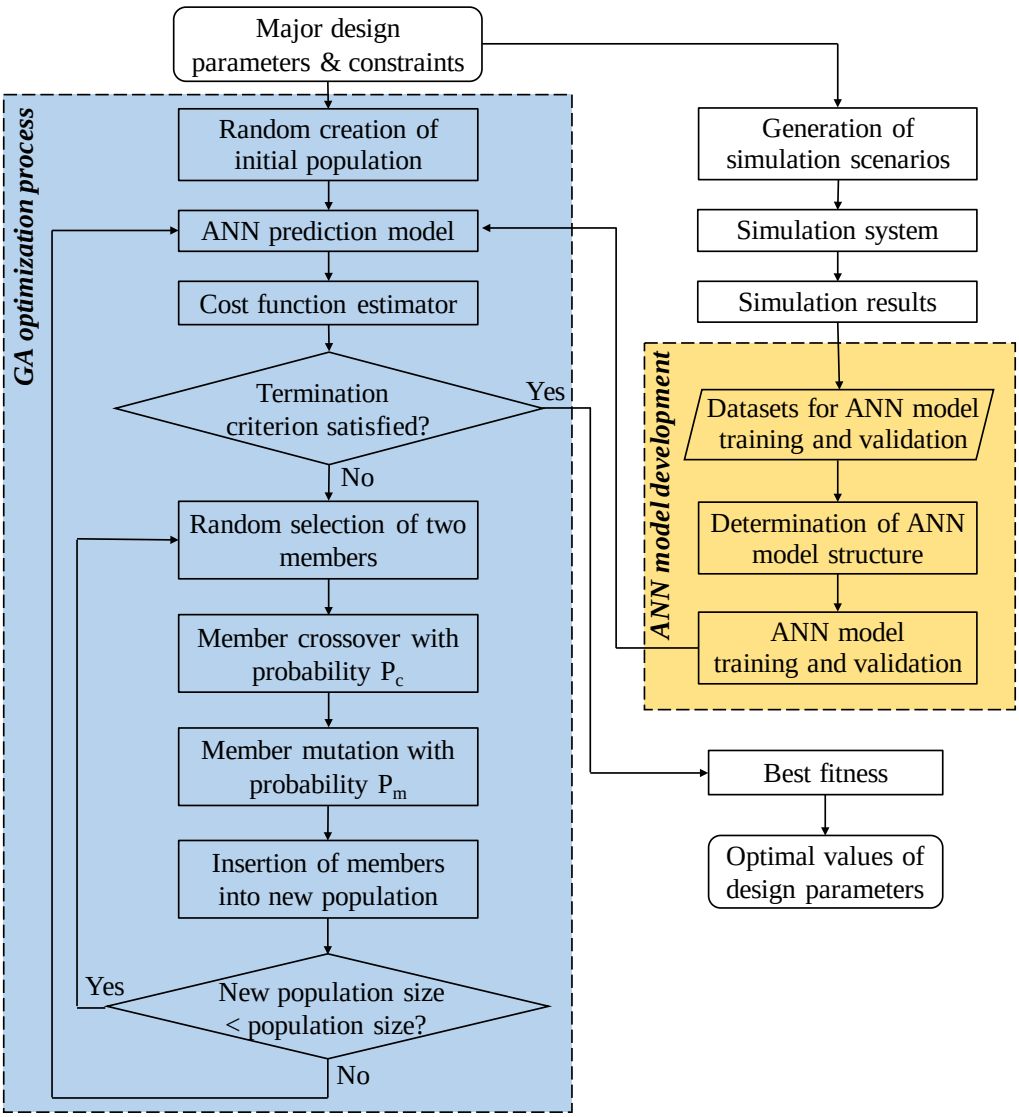

Fig. 4 Outline of the optimization strategy.

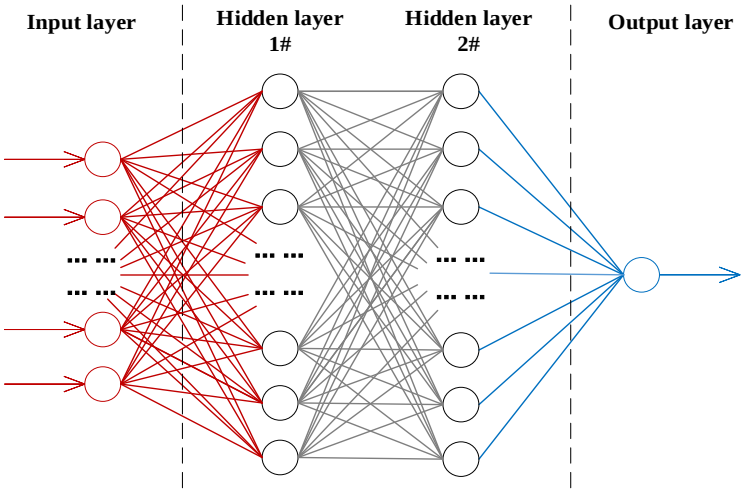

Fig. 5 Structure of the ANN model used.

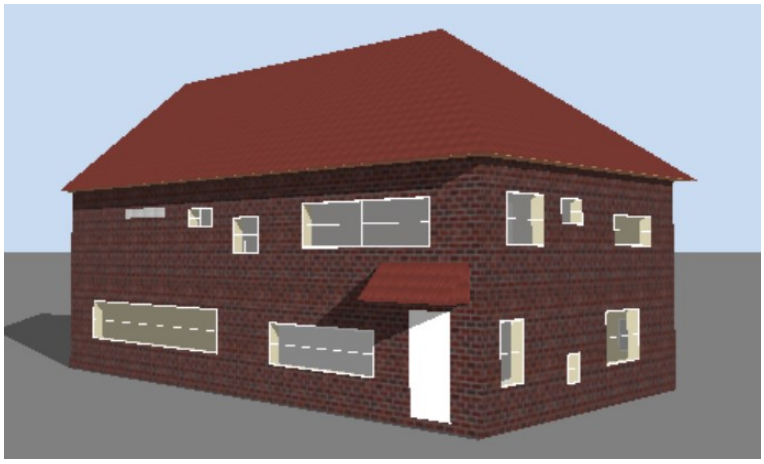

a) House model

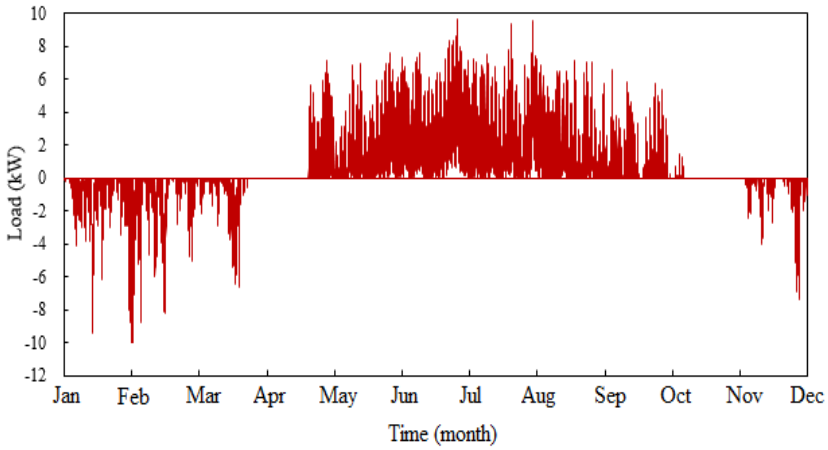

b) Simulated house load profile

Fig. 6 Illustration of the house model and the simulated load profile.

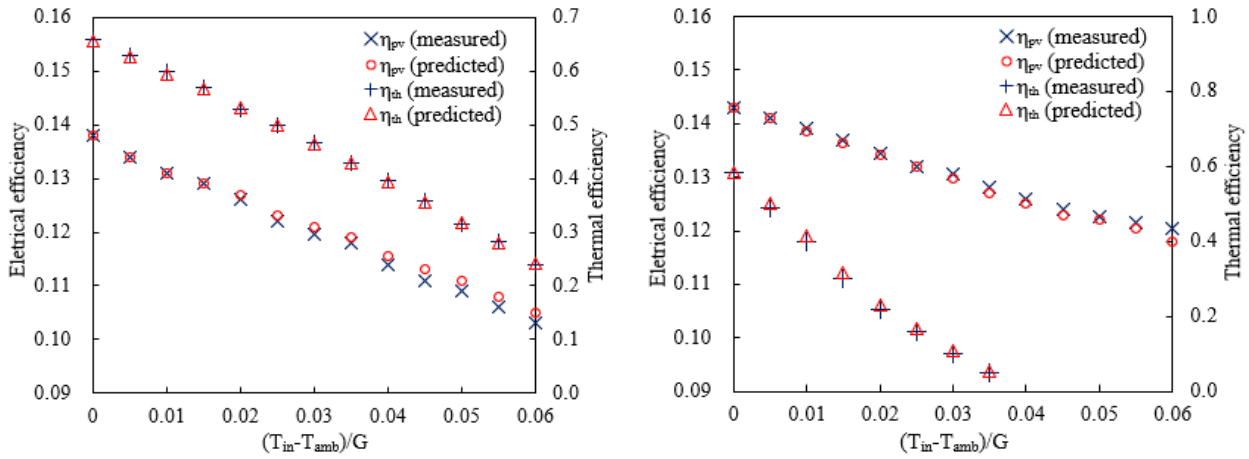

a) Glazed PVT b) Unglazed PVT

Fig. 7 Validation results of the glazed and unglazed PVT models.

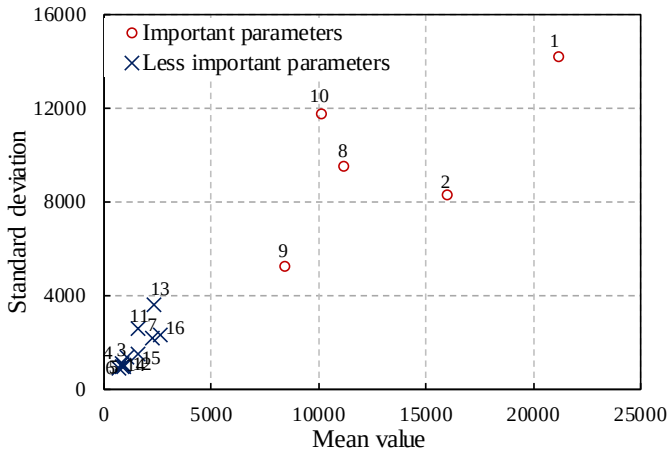

Fig. 8 Results from the Morris sensitivity analysis.

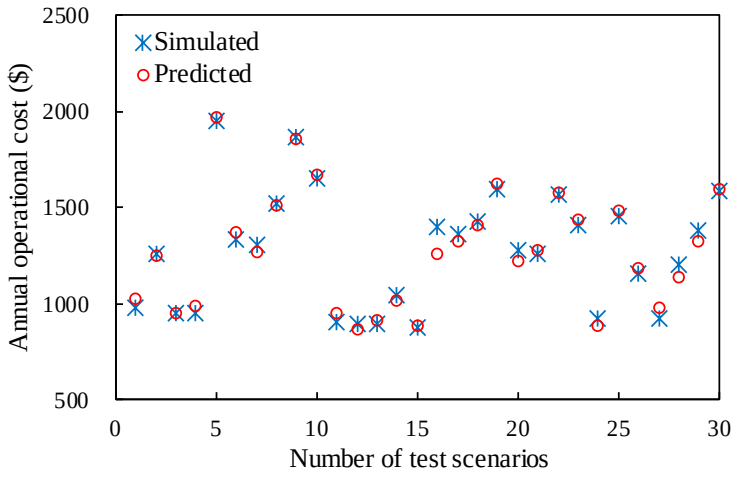

Fig. 9 Validation results of the ANN model.

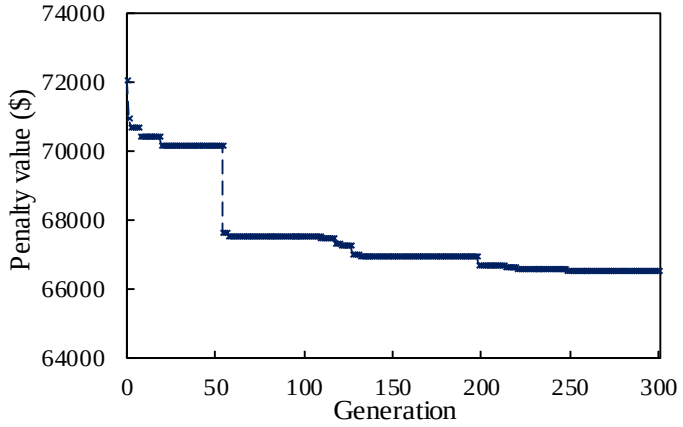

Fig. 10 Variations of the penalty value of the best individual in each generation.

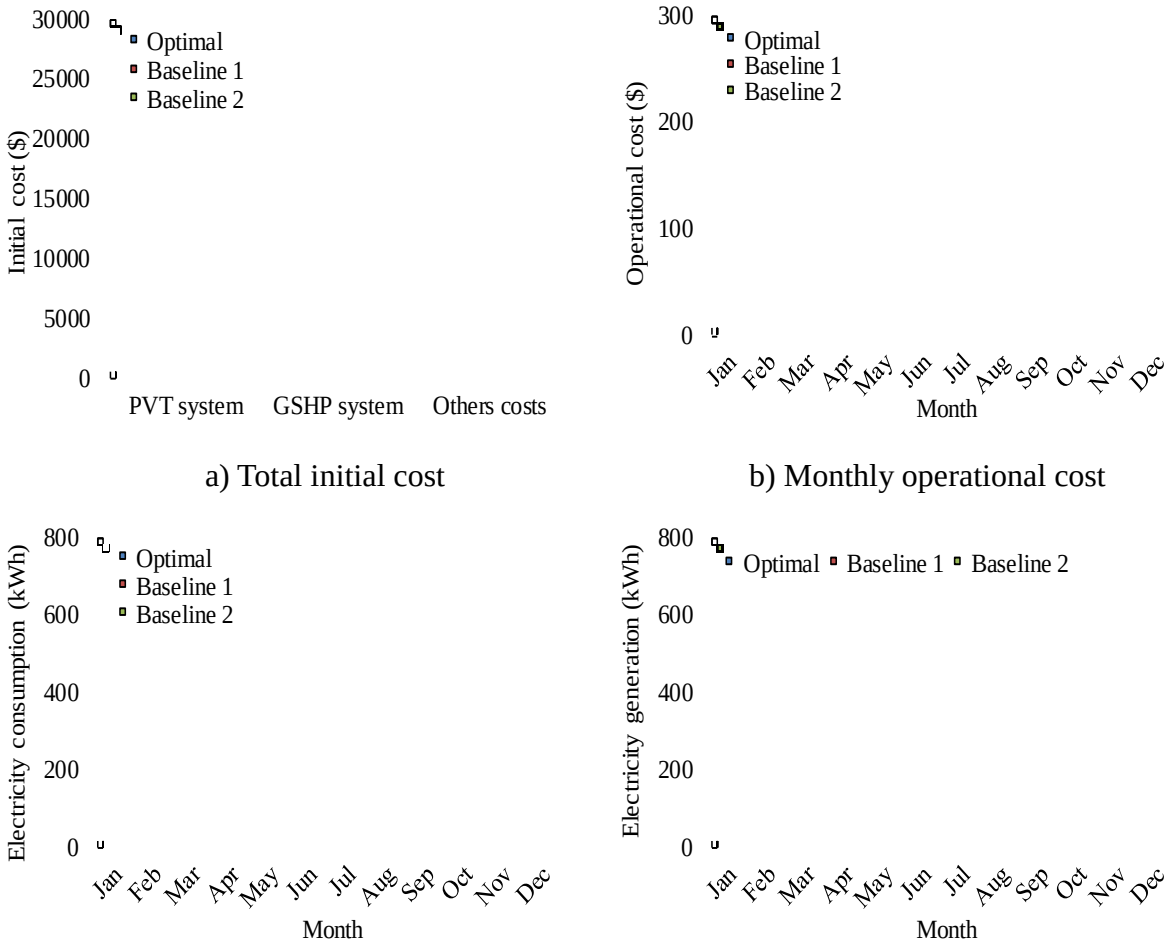

a) Total initial cost

b) Monthly operational cost

c) Monthly electricity consumption

d) Monthly electricity generation

Fig. 11 Initial cost and the annual performance of the GSHP-PVT system under the optimal and two baseline design cases.

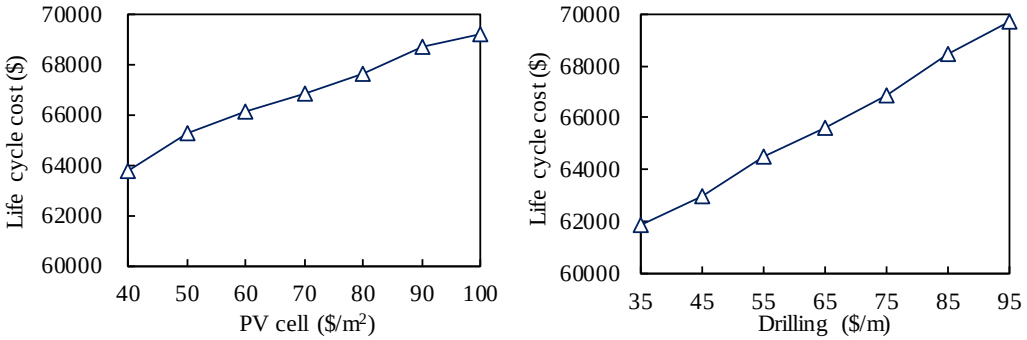

a) PV cell prices

b) Drilling costs

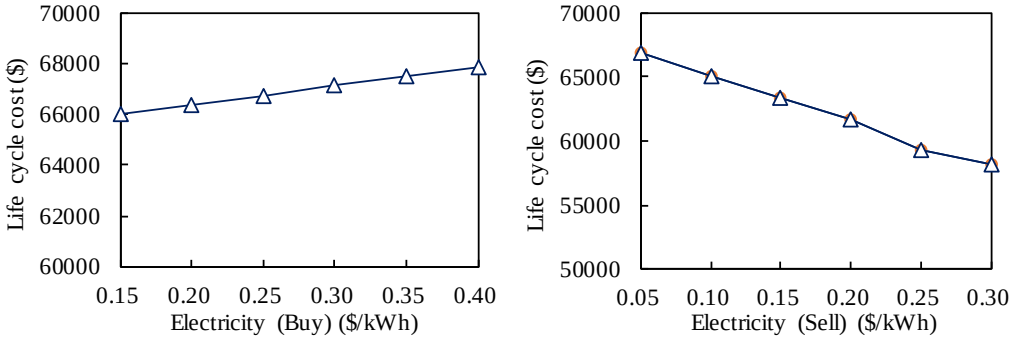

c) Electricity buy prices

d) Electricity sell prices

Fig. 12 The sensitivity of the 20-year LCC of the GSHP-PVT system to the variations in economic parameters.